# Multi-Messenger Mass–Radius Measurements and Constraints on Dense Nuclear Matter

Ang Li 李昂
liang@xmu.edu.cn
Xiamen University

Many thanks for Invitation!

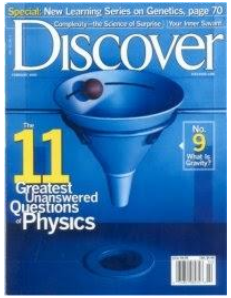
International workshop on “Origin of Elements and Cosmic Evolution” (OECE2026)
Beihang University, China, NOV 2-6, 2026

# The unknown neutron star structure: One of 11 questions of physics

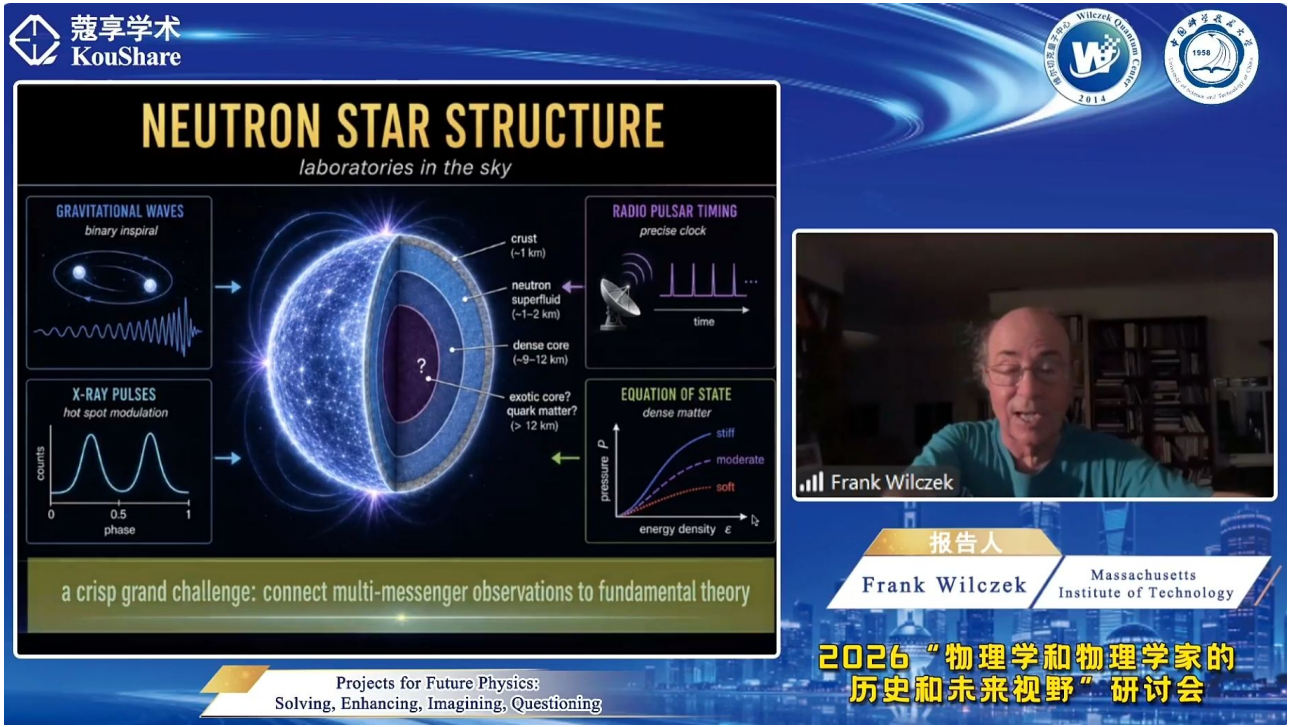
"Solving: Old Problems, Newly Ripe"

- **Neutron star structure (this talk)**
- Axion dark matter
- User-friendly superconductivity

*Our task: Connect multi-messenger observations to microscopic theory.*




Discovery
February 2002



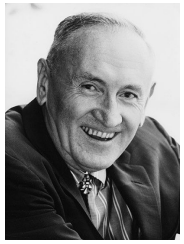

*2026 Symposium on Historical and Future Perspectives of Physics and Physicists, Shanghai, August 17–18, 2026*

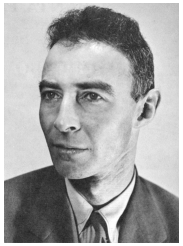
# Neutron star physical conditions and observations

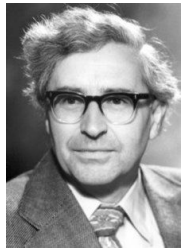

Lev Landau


James Chadwick


Walter Baade


Fritz Zwicky


J. Robert Oppenheimer


Antony Hewish
Nobel prize 1974


Dame Jocelyn Bell Burnell
Fundamental Physics Breakthrough Prize 2018

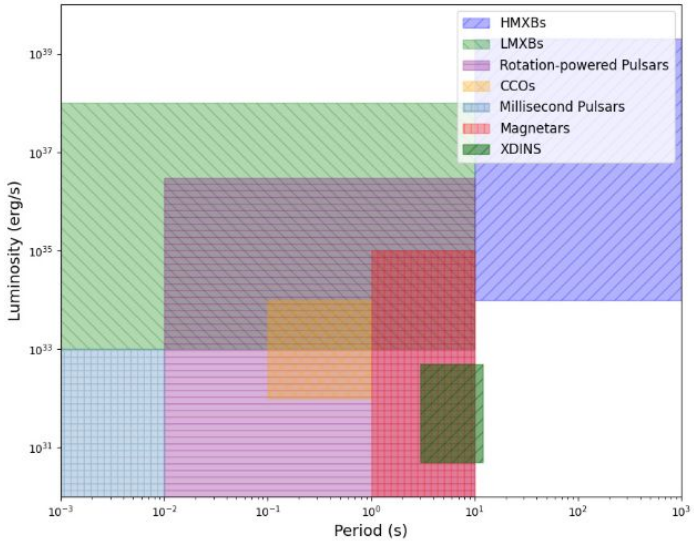
1932- 1967

*"the density of matter becomes so great that atomic nuclei come in close contact, forming one **gigantic nucleus**."*

- Rapid spin（P~$10^{-3}$-$10^{1.5}$s);
- Hot surface (T~$10^{5-6}$ K);
- Strong B field (B~$10^{8-15}$)T;
- Strong E field (ΔU~$10^{12-17}$V)

*fast rotation + strong B field -> strong E field;*
*acceleration of charged particles -> radiation;*
*energetic radiation -> pair production*

- pulsations in radio and X-ray;
- X-ray bursts;
- giant flares in magnetars;
- superbursts and thermal relaxation in accreting NSs.



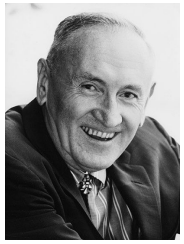

*eXTP White paper, 2506.08104 Sci. China 2025*

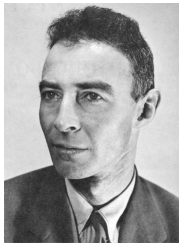
# Neutron star physical conditions and observations

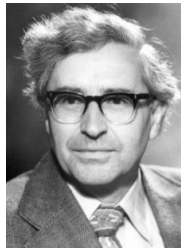

Lev Landau


James Chadwick


Walter Baade


Fritz Zwicky


J. Robert Oppenheimer


Antony Hewish
Nobel prize 1974


Dame Jocelyn Bell Burnell
Fundamental Physics Breakthrough Prize 2018

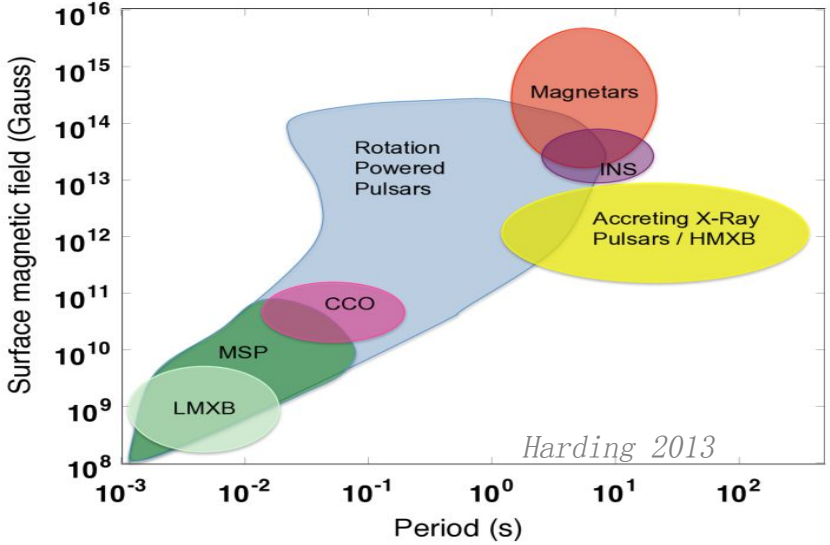
1932- 1967

*"the density of matter becomes so great that atomic nuclei come in close contact, forming one **gigantic nucleus**."*

- Rapid spin（P~$10^{-3}$-$10^{1.5}$s);
- Hot surface (T~$10^{5\text{-}6}$ K);
- Strong B field (B~$10^{8\text{-}15}$)T;
- Strong E field (ΔU~$10^{12\text{-}17}$V)

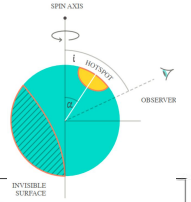
*fast rotation + strong B field -> strong E field;*
*acceleration of charged particles -> radiation;*
*energetic radiation -> pair production*

- pulsations in radio and X-ray;
- X-ray bursts;
- giant flares in magnetars;
- superbursts and thermal relaxation in accreting NSs.

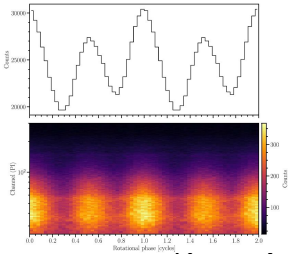


# Pulsed thermal emission caused by hot spots on a rotating MSP help measure M/R

Predict the emission received by a distant observer, assuming that it is due to one (or multiple) **hot spot(s)** on the stellar surface rotating rigidly with star;

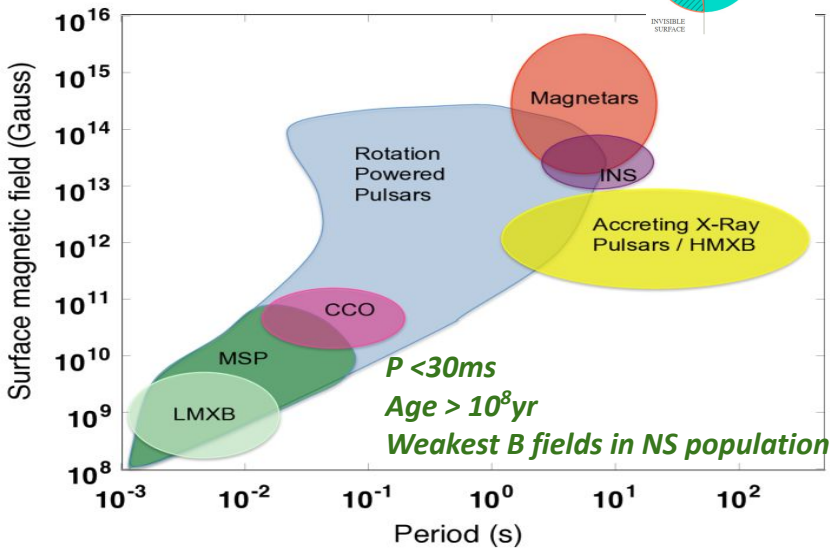



Stellar **M** controls the level of light bending;
Stellar **R** causes an asymmetry in ***pulse profile*** due to rotation:



**Primary assumption** made concerns the propagation of photons in the atmosphere, which is typically assumed to be non-magnetized and composed of fully ionized hydrogen (or helium): **Justified for MSPs;**

The asymmetry the pulse profile becomes more pronounced for **fast** rotators;




**Successfully applied to e.g., PSR J0030+0451, J0740+6620, J0437−4715, J1231−1411, J0614−332.**

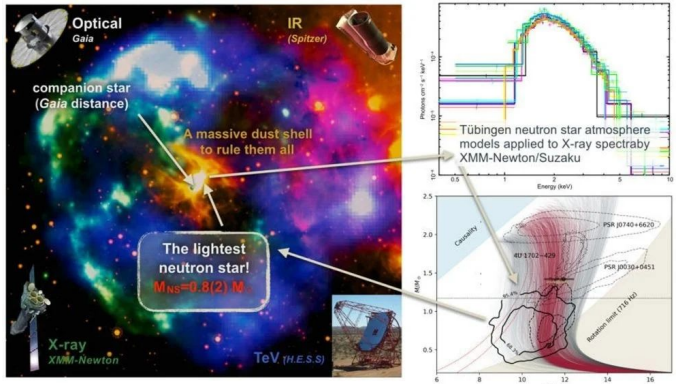
The technique is the most promising in providing accurate and precise constraints on R in the coming years!

*Ascenzi, Graber & Rea, 2401.14930*

# Simplicity of CCO energy spectra position them as excellent sources for studying the EOS

**CCOs**: Radio-quiet isolated NSs emitting steady thermal x-ray; **Low** dipolar B fields ($10^{10}$-$10^{11}$ T); Being discovered due to their locations at the centers of luminous shell-like SN remnants;

Energy spectra can be **well-fitted with thermal emissions**, even in the case of the three pulsed CCOs which exhibit non-uniform surface T;




Data from XMM-Newton + Suzaku + Gaia (**reliable D estimation**): Estimating the CCO's distance based on that of the optical star in the same shell in SN remnant HESS J1731-347, available from Gaia parallax measurements.

$$M = 0.77^{+0.20}_{-0.17} M_\odot$$

$$R = 10.4^{+0.86}_{-0.78} \text{ km}$$

*Doroshenko et al. 2022*

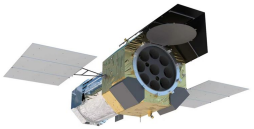
Summary of R measurement: somewhat/strongly **model-dependent**

| Method | GWs | Radio | Optical | X-ray | $\gamma$-ray |
|---|---|---|---|---|---|
| Surface emission spectral modeling | | | | | |
| Photospheric radius expansion | | | | | |
| X-ray lightcurve modeling | | | | | |
| NS-BH merger + GRB | | | | | |
| GW asteroseismology | | | | | |

*Note: the systematics and physical assumptions behind the HESS J1731 measurements are HUGE.*

*Ascenzi, Graber & Rea, 2401.14930*

# NS-LMXB outburst+quiescence: Burst, QPO, cooling for M-R study



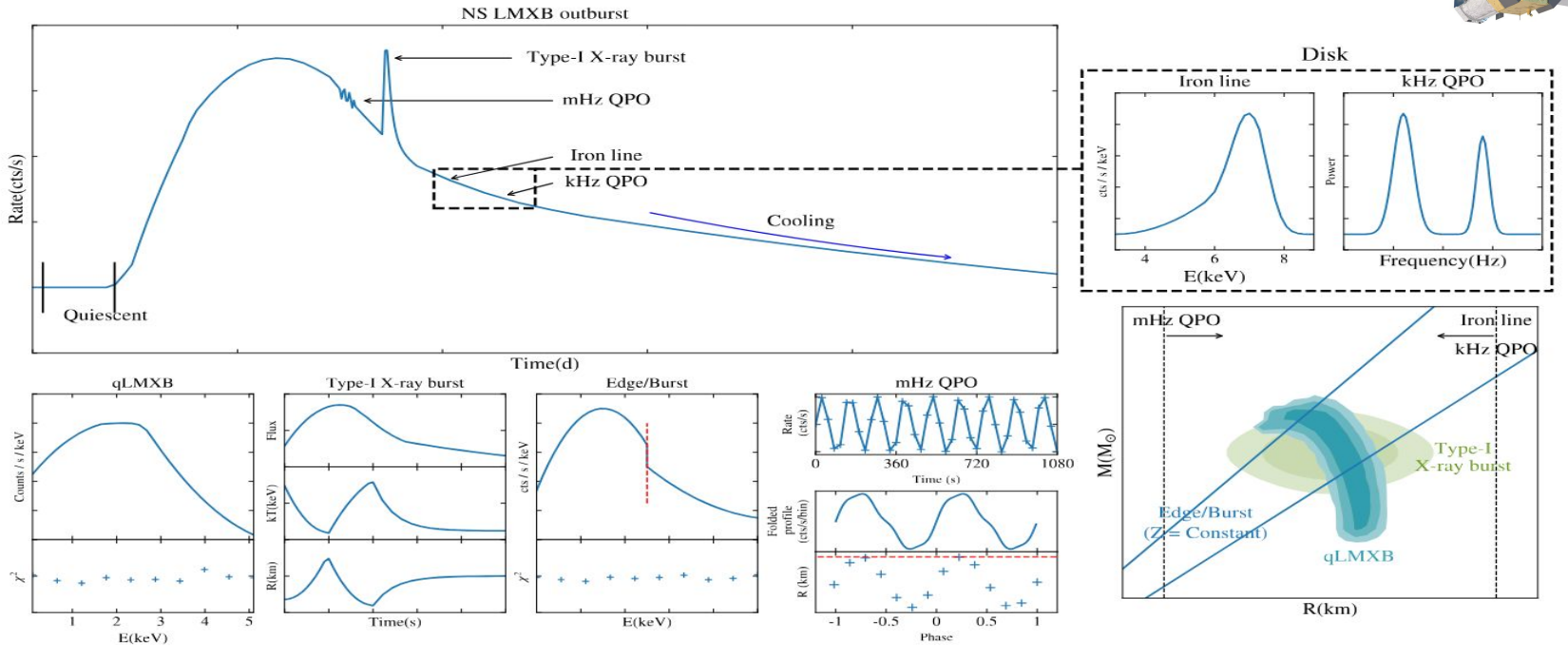



**Figure 8** This schematic illustrates key observational and temporal features of a NS-LMXB system during outburst and quiescent phases. Upper Left Panel:

*eXTP White paper, 2506.08104*

*Sci. China 2025*

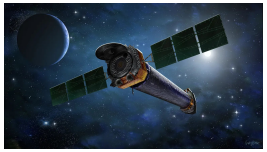
# EXO 0748−676: Measurement summary

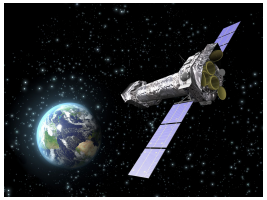
- EXO 0748−676 is a well-known LMXB system located in the constellation Pisces, approximately 7.4 kpc (about 24,000 light-years) from Earth;
- The system consists of a neutron star and a low-mass companion star (optical counterpart: UY Vol).

| Method | $M$ ($M_\odot$) | $R$ (km) | Reference |
|---|---|---|---|
| Gravitational redshift ($z = 0.35$) | 1.4–1.8 | 9–12 | Cottam et al. (2002) |
| Eddington limit + redshift + cooling tail | $2.10 \pm 0.28$ | $13.8 \pm 1.8$ | Özel (2006) |
| Dynamical constraints | $> 1.5$ | — | Muñoz-Darias et al. (2009) |
| *XMM* spectral fitting (`nsagrav` / `nsatmos`) | $1.77 \pm 0.45 / 1.71 \pm 0.30$ | $16.6^{+1.8}_{-7.5} / 16.5 \pm 0.5$ | Zhang et al. (2011) |
| *XMM* spectral fitting | $1.78^{+0.4}_{-0.6}$ | $13.7^{+1.0}_{-2.7}$ | Díaz Trigo et al. (2011) |
| Optical spectroscopy | $> 1.27$ | — | Ratti et al. (2012) |
| *Chandra* spectral fitting | $1.64 \pm 0.38$ | $13.2^{+0.6}_{-2.0}$ | Degenaar et al. (2014) |
| *XMM* spectral fitting (0.3–10 / 0.5–10 keV) | $2.08^{+0.07}_{-0.15} / 1.50^{+0.40}_{-0.99}$ | $11.9 \pm 0.7 / 12.2^{+1.0}_{-3.6}$ | Cheng et al. (2017) |
| Eclipse mapping (Gaussian/Exponential density profile) | $2.01^{+0.22}_{-0.21} / 2.02^{+0.29}_{-0.27}$ | — | Knight et al. (2022) |
| Quiescent spectral fitting (*Chandra*+*XMM*; `nsatmos`) | $1.77^{+0.17}_{-0.22}$ | $12.62^{+0.56}_{-0.74}$ | This work (distance $\simeq 7.1$ kpc) |

*2606. 23466*

# The observational dataset





*2606. 23466*

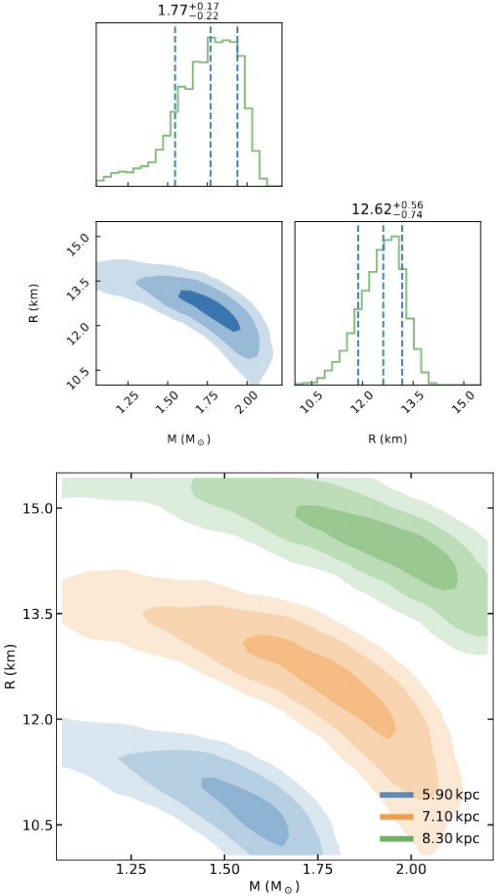
**Table 1.** Chandra and XMM-Newton observations of EXO 0748−676 used in this work.

| Instr. | ObsID | Date | MJD | Detector | Exposure (ks) |
|---|---|---|---|---|---|
| Chandra | 9070 | 2008-10-12 | 54751 | ACIS-S | 13.77 |
| Chandra | 10873 | 2008-10-15 | 54754 | ACIS-S | 13.29 |
| XMM-Newton | 0560180701 | 2008-11-06 | 54776 | MOS1/MOS2/PN | 29.52/29.52/27.93 |
| Chandra | 9071 | 2009-02-23 | 54885 | ACIS-S | 15.83 |
| Chandra | 10871 | 2009-02-25 | 54887 | ACIS-S | 9.58 |
| XMM-Newton | 0605560401 | 2009-03-18 | 54908 | MOS1/MOS2/PN | 43.82/42.67/41.91 |
| Chandra | 9072 | 2009-06-10 | 54992 | ACIS-S | 27.22 |
| XMM-Newton | 0605560501 | 2009-07-01 | 55013 | MOS1/MOS2/PN | 101.62/101.62/100.03 |
| Chandra | 11059 | 2010-04-20 | 55306 | ACIS-S | 27.37 |
| XMM-Newton | 0651690101 | 2010-06-17 | 55364 | MOS1/MOS2/PN | 98.87/98.89/96.40 |
| Chandra | 11060 | 2010-10-20 | 55489 | ACIS-S | 27.22 |
| Chandra | 12414 | 2011-07-02 | 55744 | ACIS-S | 38.07 |
| XMM-Newton | 0690330101 | 2013-04-15 | 56397 | MOS1/MOS2/PN | 104.07/104.12/102.54 |
| Chandra | 14663 | 2013-08-01 | 56505 | ACIS-S | 42.86 |
| XMM-Newton | 0824420101 | 2018-05-02 | 58240 | MOS1/MOS2/PN | 77.62/77.60/75.76 |
| Chandra | 23440 | 2021-08-03 | 59429 | ACIS-S | 26.83 |
| Chandra | 24516 | 2021-09-21 | 59478 | ACIS-S | 23.60 |
| Chandra | 30047 | 2025-05-23 | 60818 | ACIS-S | 14.14 |
| Chandra | 30048 | 2025-06-17 | 60843 | ACIS-S | 18.43 |
| Chandra | 30049 | 2025-08-11 | 60898 | ACIS-S | 23.50 |

# EXO 0748−676: New Quiescent X-ray M–R Constraints

- Dataset (2008–2025, two quiescent epochs)
  - 14 **Chandra** ACIS-S + 6 **XMM-Newton** (MOS/PN) observations
  - Two quiescent intervals bracketing the 2024–2025 outburst
- Spectral model & MCMC setup
  - Global fit: tbabs*(nsatmos+powerlaw) in 0.5–10 keV
  - **Tied across all 20 spectra: M, R, NH;** epoch-dependent photon index Γ; Teff and power-law normalization per observation
- Baseline mass–radius result (D = 7.1 kpc)
  - Posterior: **M = 1.77**$^{+0.17}_{-0.22}$**M⊙ R = 12.62**$^{+0.56}_{-0.74}$ **km** (1σ credible intervals)
- Explicit tests of distance (right figure), atmosphere, and spectral assumptions
- Combined with dynamical lower limits ($M \gtrsim 1.5\ M_\odot$) and NICER/GW systematics, EXO 0748−676 supports relatively **stiff** dense-matter EOSs

*2606. 23466*

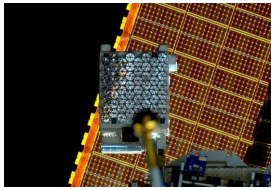


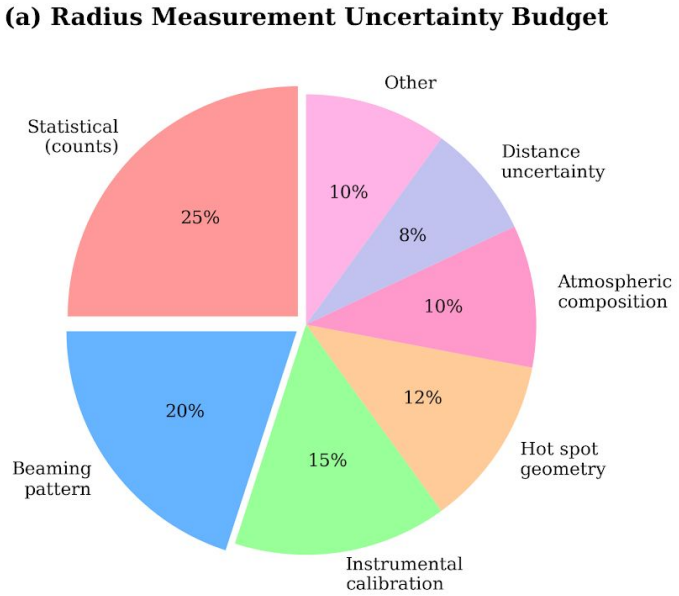
# Outline

- Intro. on neutron stars and M, R study
- **Observations** and multi-messenger constraints
- Prospects and opportunities

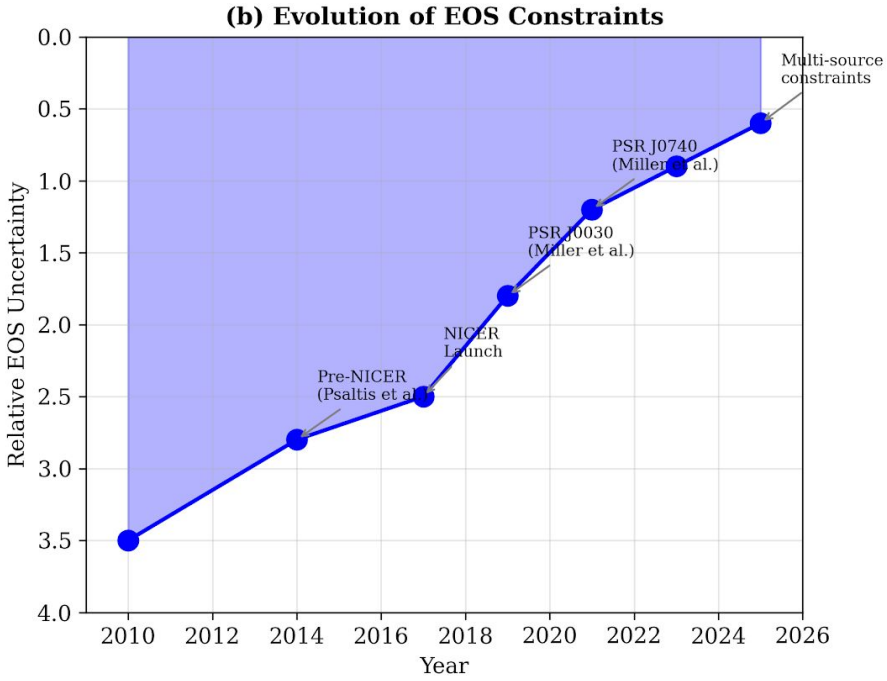
# Uncertainty budget for NICER radius measurements

Neutron star pulse profile modeling has matured from a theoretical possibility to a **precision measurement technique**, enabled by the combination of large collecting area, excellent timing resolution, and soft X-ray sensitivity, e.g., NICER (2017), **eXTP(2030)**, NewATHENA (~2038)





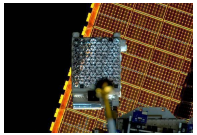

*AI-generated figure*

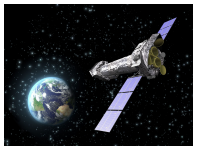


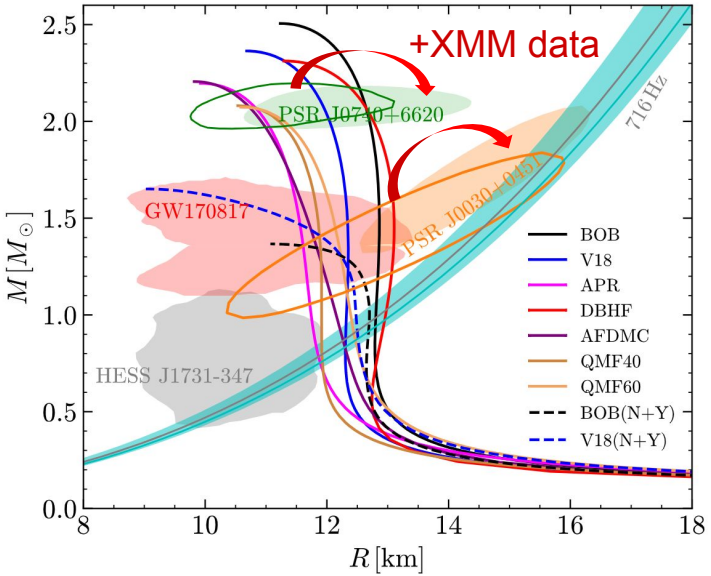
# Why background information is important

XMM-Newton data can provide (indirect) NICER background constraint:
The introduction of the XMM-Newton data (EPIC MOS1 and MOS2) led to a **reduction in background estimates from NICER-only data,** resulting in higher compactness value:

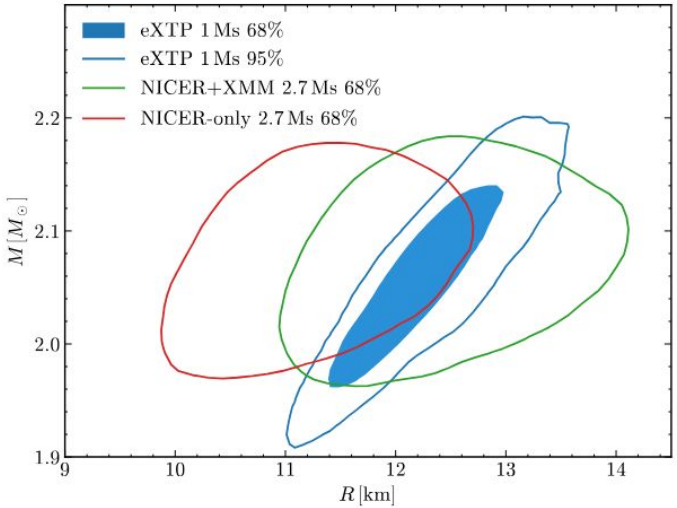









2402.02799




Radius measurement precision～5% with eXTP-SFA

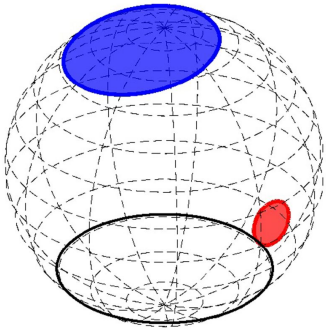
*eXTP White paper, arXiv:2506.08104 Sci. China 2025*

**Figure 4** 2-D marginalized posteriors of mass and radius of PSR J0740+6620, reconstructed from the simulated pulse profiles observed

# Geometric information matters: PSR J0437-4715 as an example

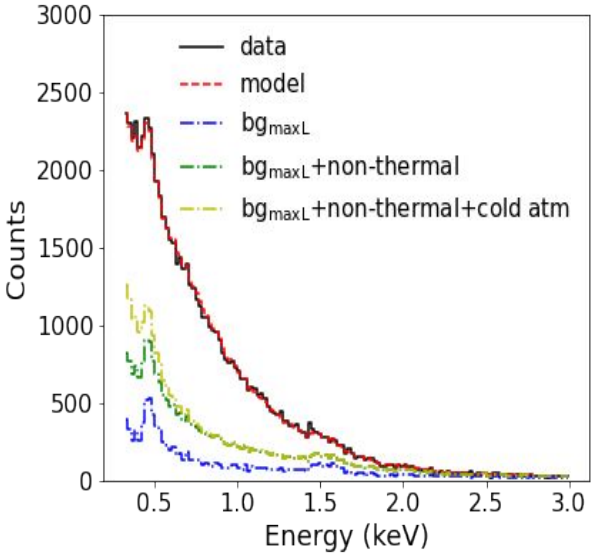
- Polarization data play a crucial role in resolving hot-spot geometric degeneracy;
- Distinguish among three emission components: thermal radiation from NS cold surface, thermal emission from polar hotspots, and nonthermal power-law emission, possibly originating in the magnetosphere;
- Multi-component emission in the broadband spectrum spanning the far-ultraviolet and X-ray bands.

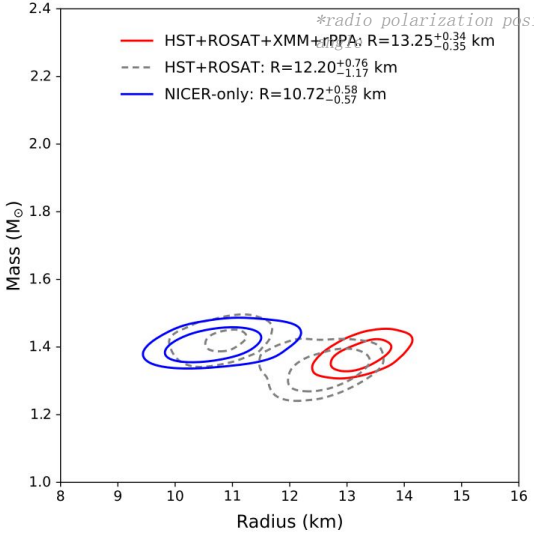
*2605.05429*



- Best-fit parameters:

→ Bulk surface temperature: ~$2.1\times10^5$ K
→ Hot-spot temperature: ~$1.2\times10^6$ K
→ Hot-spot geometries: radio-consistent
→ Non-thermal: $\Gamma_{PL} \approx 2.3$



# eXTP Synergy: Large Area + Polarimetry + Timing

**The enhanced X-ray Timing and Polarimetry mission—eXTP for launch in 2030**

Zhang, Shuang-Nan; Santangelo, Andrea; Xu, Yupeng; Feng, Hua; Lu, Fangjun; Ch
2025/09 · Science China Physics, Mechanics, and Astronomy · **cited: 62**
Volume: 68 · Page/ID: 119502

**Physics of strong magnetism with eXTP**

Ge, Mingyu; Ji, Long; Taverna, Roberto; Tsygankov, Sergey; Xu, Yanjun; Sant
2025/09 · Science China Physics, Mechanics, and Astronomy · **cited: 22**
Volume: 68 · Page/ID: 119505

**Dense matter in neutron stars with eXTP**

Li, Ang; Watts, Anna L.; Zhang, Guobao; Guillot, Sebastien; Xu, Yanjun; Santangelo,
2025/09 · Science China Physics, Mechanics, and Astronomy · **cited: 54**
Volume: 68 · Page/ID: 119503

**Probing the strong gravity region of black holes with eXTP**

Bu, Qingcui; Bambi, Cosimo; Gou, Lijun; Xu, Yanjun; Uttley, Phil; De Rosa, Ales
2025/09 · Science China Physics, Mechanics, and Astronomy · **cited: 9**
Volume: 68 · Page/ID: 119504

**Prospects for time-domain and multi-messenger science with eXTP**

Yi, Shu-Xu; Zhao, Wen; Xu, Ren-Xin; Wu, Xue-Feng; Stratta, Giulia; Dall'Osso, Simone
2025/09 · Science China Physics, Mechanics, and Astronomy · **cited: 10**
Volume: 68 · Page/ID: 119506

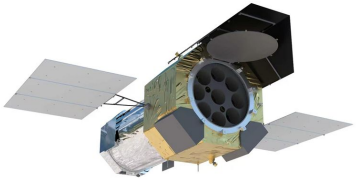
**Observatory science with eXTP**

Zhou, Ping; Mao, Jirong; Zhang, Liang; Patruno, Alessandro; Bozzo, Enrico;
2025/09 · Science China Physics, Mechanics, and Astronomy · **cited: 17**
Volume: 68 · Page/ID: 119507

| Parameter | Value |
|---|---|
| Orbit | Apogee>100000km, perigee 5000km, Earth's highly elliptical orbit. |
| inclination | 28° |
| Pointing | 3-axis stabilized, < 3" (3σ) |
| Launch | LM3B, from XiChang |
| Launch mass | ~4000 kg |
| Telemetry | 1.7 Tb/2 day (Ku-band) |
| Mission duration | 5 years (goal 8 years) |
| Launch date | ~ Jan. 2030 |

Reads

| | Totals | Refereed |
|---|---|---|
| Total number of reads | 2253 | 2253 |
| Average number of reads | 375.5 | 375.5 |
| Median number of reads | 405 | 405 |
| Total number of downloads | 1041 | 1041 |
| Average number of downloads | 173.5 | 173.5 |
| Median number of downloads | 186 | 186 |



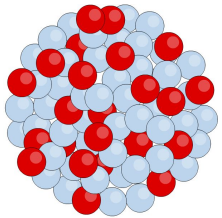
Key Science Goals:

- Determine the EOS of ultra-dense matter in neutron stars;
- Measure mass-radius relations via pulse profile modeling, burst oscillations, and polarization;
- Study QED effects in strong magnetic fields (10^{13}–10^{15} G);
- Probe accretion physics and dynamics in strong gravity

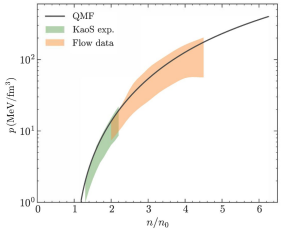
# Bayesian EOS Inference Framework

**1. Model for interaction between particles**

$\hat{\mathcal{H}}\Psi = E\Psi$



**2. EOS prior pasting test**




$G_{\mu\nu} = \frac{8\pi G}{c^4} T_{\mu\nu}$

**3. EOS inference from NS obs. (GW, photons, neutrinos)**

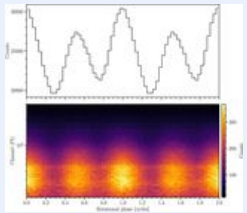
Posterior

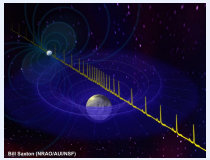
$p(\boldsymbol{\theta}|D,\mathbb{M})$

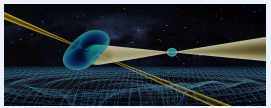
Parameter Data Mod

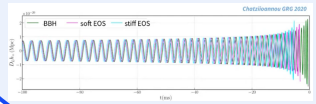
**Physics on the EOS, the composition and the underlying strong interaction**

This multi-messenger approach combining GW, EM observations, and terrestrial experiments, provides the most robust constraints on the EOS of dense matter.



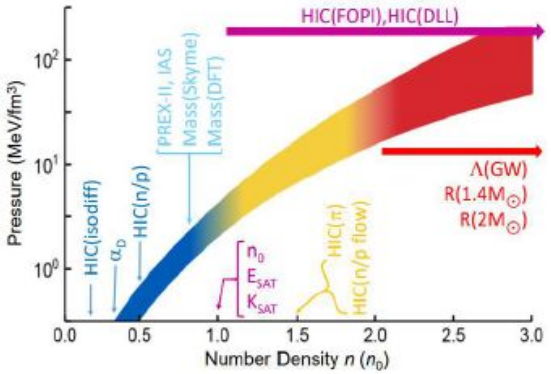




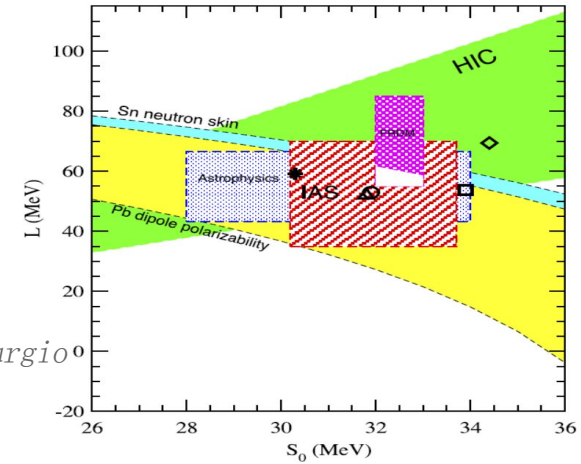


# Laboratory Constraints: HICs & Finite Nuclei

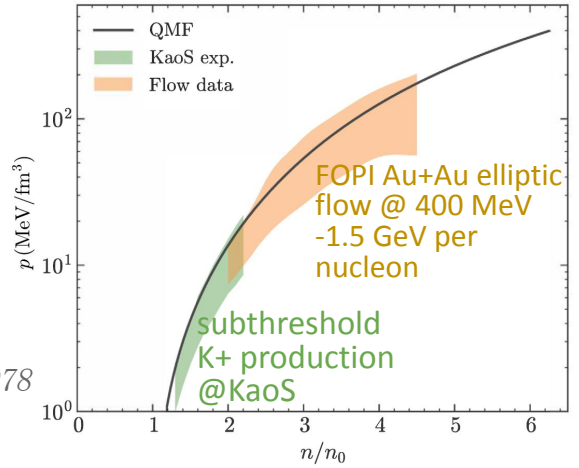
- Finite nuclei
  - Masses, radii, polarizability, neutron-skin thickness →$K_0$, $S_0$, L
- Intermediate-energy heavy-ion collisions (HICs)
  - Constrain pressure at ρ ≈ (1–2) $\rho_0$
- Role in this talk
  - Set low-density pressure band that EOSs must pass through
  - Provide independent checks on symmetry energy behavior




*Kumar et al. (FRIB)*




*Baldo & Burgio PPNP 2016*




*2211.04978*

# Testing the phase transition parameters inside neutron stars with the production of protons and lambdas in relativistic heavy-ion collisions

Ang Li,[1,*] Gao-Chan Yong,[2,3] and Ying-Xun Zhang[4,5]

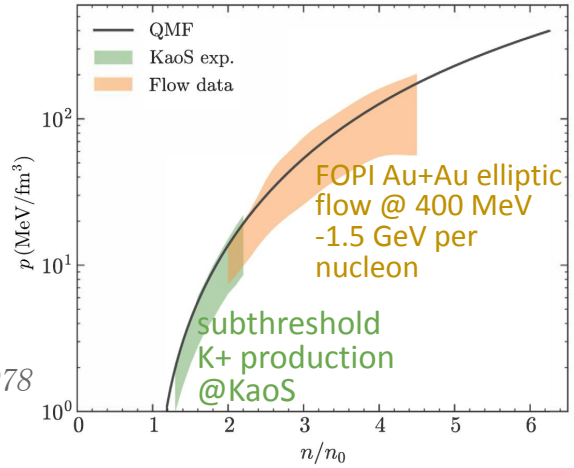
[1]*Department of Astronomy, Xiamen University, Xiamen, Fujian 361005, China*
[2]*Institute of Modern Physics, Chinese Academy of Sciences, Lanzhou 730000, China*
[3]*School of Nuclear Science and Technology, University of Chinese Academy of Sciences, Beijing 100049, China*
[4]*China Institute of Atomic Energy, Beijing 102413, China*
[5]*Guangxi Key Laboratory Breeding Base of Nuclear Physics and Technology, Guilin 541004, China*

(Received 18 November 2022; accepted 9 January 2023; published 6 February 2023)

We demonstrate the consistency of the quark deconfinement phase transition parameters in the beta-stable neutron star matter and in the nearly symmetric nuclear matter formed in heavy-ion collisions (HICs). We investigate the proton and $\Lambda$ flow in Au + Au collisions at 3 and 4.5 GeV/nucleon incident beam energies with the pure hadron cascade version of a multiphase transport model. The phase transition in HICs and neutron stars is described based on a class of hybrid equations of state from the quark mean-field model for the hadronic phase and a constant-speed-of-sound parametrization for the high-density quark phase. The measurements of the anisotropic proton flow at 3 GeV/nucleon by the STAR Collaboration favor a relatively low phase transition density lower than ~2.5 times saturation density indicated by the gravitational wave and electromagnetic observations of neutron stars. And the proton flow data at the higher energy of 4.5 GeV/nucleon can be used to effectively constrain the softness of high-density quark matter equations of state. Finally, compared to the proton flow, the $\Lambda$ flow is found to be less sensitive and not constraining to the equations of state.

DOI: 10.1103/PhysRevD.107.043005

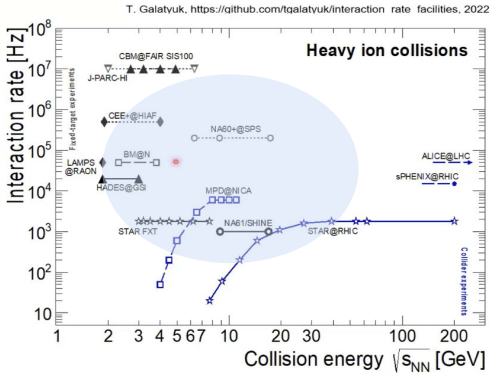
*2211. 04978*



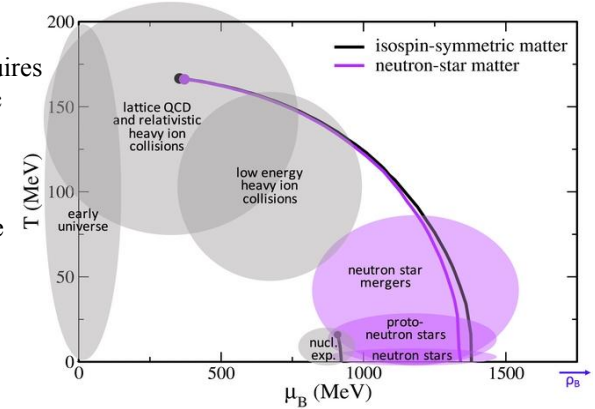
# One dense-matter program: stars, laboratories, and inference

- Heavy-ion collisions involve **hot, transient, often approximately isospin-symmetric** matter,
- Neutron stars contain cold, highly neutron-rich, beta-equilibrated matter.

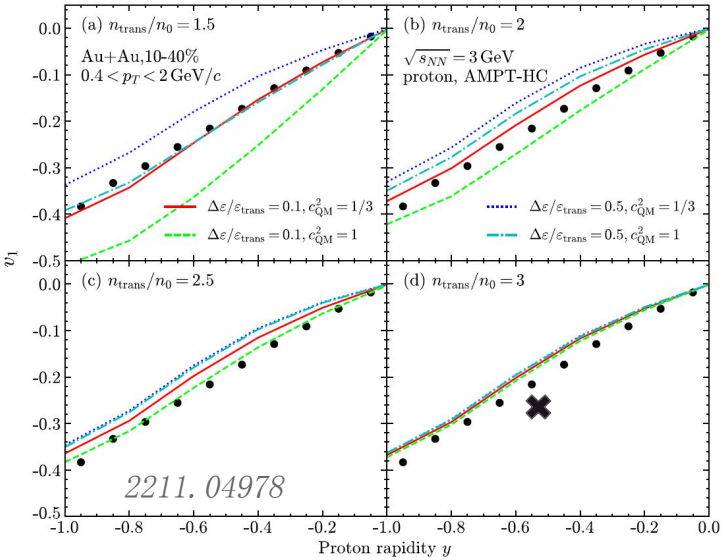
Experiments at facilities such as HIAF, FAIR, RHIC, NICA, and RIKEN probe different regions of the nuclear phase diagram:




A direct comparison therefore requires a microscopic model that consistently translates between these conditions.




Two colliding nuclei produce collective motion of nucleons and fragments, depends sensitively on the gradient of pressure (i.e., **soft/stiff EOS**); Example result favor a relatively low **phase transition** density <~2.5$n_0$, similar to NS obs:



## In-medium effects of nucleon-nucleon cross sections in heavy-ion collisions

Shuochong Han,[1,2] Xinle Shang,[2,3,*] Wei Zuo,[2,3] Gaochan Yong,[2,3] and Ang Li[1]
[1]*Department of Astronomy, Xiamen University, Xiamen, Fujian 361005, China*
[2]*Institute of Modern Physics, Chinese Academy of Sciences, Lanzhou 730000, China*
[3]*School of Nuclear Science and Technology, University of Chinese Academy of Sciences, Beijing 100049, China*

(Received 20 October 2025; revised 12 March 2026; accepted 22 May 2026; published 6 July 2026)

Based on the isospin-dependent Boltzmann-Uehling-Uhlenbeck transport model, we systematically investigate the in-medium effects of nucleon-nucleon ($NN$) cross sections on nucleonic and pionic observables in heavy-ion collisions, employing microscopic cross sections derived from the Brueckner-Hartree-Fock approach. Key observables include nuclear stopping, the neutron-to-proton ($n/p$) ratio, neutron-proton transverse flow differences, differential collective flow, pion multiplicities, and the resulting $(\pi^-/\pi^+)_{\rm like}$ ratio. The analysis disentangles the respective contributions from the scattering amplitude, the density of states, and the total momentum ($K$) of the colliding pairs. We find that larger in-medium $NN$ cross sections generally enhance free nucleon emission and nuclear stopping with the nucleon effective mass playing a dominant suppressive role. However, it is insufficient to account only for the medium corrections from effective mass: both the medium effect from the scattering amplitude and the $K$ dependence exert noticeable influences on the observables. In particular, nuclear stopping is found to be highly sensitive to these in-medium modifications of cross sections. While the $n/p$ ratio and transverse flow difference remain largely insensitive, the differential collective flow and pion yields are strongly affected. These results indicate that the interplay between scattering amplitude, density-of-states and $K$ dependence is essential to accurately describe medium effects in heavy-ion collisions.



## Bayesian analyses of proton multiple flow components in intermediate heavy ion collisions with momentum-dependent interactions

Shuochong Han and Ang Li*
*Department of Astronomy, Xiamen University, Xiamen 361005, China*

(Received 29 September 2025; revised 20 November 2025; accepted 27 January 2026; published 13 February 2026)

We perform a comprehensive Bayesian analysis of Au + Au collision data at 1.23 GeV/nucleon using an isospin-dependent Boltzmann-Uehling-Uhlenbeck transport model that incorporates a momentum-dependent mean field and medium-modified baryon-baryon cross sections. The model parameters are calibrated to empirical properties of nuclear matter at saturation density, with particular attention to variations in the incompressibility $K_0$. Within a Bayesian statistical framework and using a Gaussian Process emulator, we simultaneously extract constraints on the incompressibility $K_0$ and the in-medium baryon-baryon scattering modification factor $X$ by systematically comparing model predictions with HADES measurements of proton collective flow, including the slopes ($F_1$ and $F_3$) of directed and triangular flow, as well as elliptic ($v_2$) and quadrupole ($v_4$) flow observables. We find that the extracted incompressibility favors relatively small values, indicating a soft nuclear equation of state, while the inferred average $X$ values fall at 0.9–1.0, suggesting mild suppression of baryon-baryon cross sections in the medium. Furthermore, we demonstrate that transport models employing momentum-independent mean fields require stiffer equations of state and stronger in-medium corrections to reproduce the same observables. These results highlight the critical role of momentum dependence in the mean field and its interplay with in-medium scattering in constraining the properties of dense nuclear matter from heavy ion collisions.

中国科学：物理学 力学 天文学 2026年 第56卷 第7期：272010
SCIENTIA SINICA Physica, Mechanica & Astronomica physcn.scichina.com
《中国科学》杂志社 SCIENCE CHINA PRESS
论文 中子星与核物质状态方程专题

# “天-地”联合限制致密物态

孙向东[1], 刘洋阳[2], 李昂[1*], 肖志刚[3], 张英逊[2*]

1. 厦门大学物理科学与技术学院, 厦门 361005
2. 中国原子能科学研究院中国核数据中心, 北京 104203
3. 清华大学物理系, 北京 100084
*联系人, 李昂, E-mail: liang@xmu.edu.cn; 张英逊, E-mail: zhyx@ciae.ac.cn

收稿日期: 2025-05-13; 接受日期: 2025-06-10; 网络出版日期: 2026-02-03
科技部SKA专项(编号: 2020SKA0120300)和国家自然科学基金(编号: 12273028, 12494572, 12205377)资助

**摘要** 当前, 精准约束致密物质的状态方程是核物理与天体物理交叉领域的前沿难题. 为突破理论与实验的局限, 本工作基于地面核物理实验中获得的核子相互作用信息, 结合核多体理论与非平衡输运模型, 并依托高精度中子星观测数据, 约束中子星核心区域致密核物质的基本性质. 具体而言, 我们自洽整合了重离子碰撞中的集体流与$\pi$介子观测数据, 以及中子星的质量、半径与潮汐形变等天文观测, 开展联合分析. 通过多维数据的贝叶斯联合统计研究, 我们获得了核饱和密度处关键状态方程参数的最新约束($1\sigma$置信区间): 不可压缩系数$K_0 = 250.56^{+16.51}_{-18.79}$ MeV, 核子有效质量比值$m^*/m = 0.6^{+0.01}_{-0.01}$, 对称能$S_0 = 28.46^{+4.36}_{-2.24}$ MeV, 以及对称能斜率$L_0 = 64.59^{+13.25}_{-9.38}$ MeV. 此外, 本工作还探讨了对上述物理量最具敏感性的可观测量, 为未来更高精度地联合地面实验与天文观测提供了有益参考与理论支持.

**关键词** 中子星状态方程, 重离子碰撞, 多信使天文学

**PACS:** 26.60.Kp, 21.65.Ef, 26.60.Dd, 25.70.-z, 97.60.Jd, 04.30.Tv

**表 1** 本文所使用的HIC观测量实验数据来源: 集体流数据来自ASY-EOS实验组[82], $\pi$介子产额及比值数据来自FOPI实验组[84]

**Table 1** Experimental data for the HIC observables used in this work: collective flow data are taken from the ASY-EOS collaboration [82], and pion yields and ratios are from the FOPI collaboration [84]

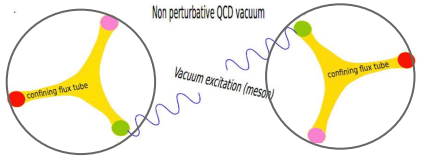
| 观测量 | 快度$y_0$ | 极角$\theta$ | 碰撞参数$b$ (fm) | 实验数据 |
|---|---|---|---|---|
| $v_1^n(p_t/A)$ | −0.5–0.5 | 37°–53° | 5.69 | ASY-EOS[82] |
| $v_1^{ch}(p_t/A)$ | −0.5–0.5 | 37°–53° | 5.69 | ASY-EOS[82] |
| $v_2^n(p_t/A)$ | −0.5–0.5 | 37°–53° | 5.69 | ASY-EOS[82] |
| $v_2^{ch}(p_t/A)$ | −0.5–0.5 | 37°–53° | 5.69 | ASY-EOS[82] |
| $v_2^n/v_2^{ch}(p_t/A)$ | −0.5–0.5 | 37°–53° | 5.69 | ASY-EOS[82] |
| $M(\pi)$ | 全快度 | 全极角 | < 2 | FOPI[84] |
| $\pi^-/\pi^+$ | 全快度 | 全极角 | < 2 | FOPI[84] |

# Outline

- Intro. on neutron stars and M, R study
- Observations and **multi-messenger constraints**
- Prospects and opportunities

# Prepare priors for a set of EOS parameters

***Step 1: Dirac equation for the quark inside nucleon;***




$$[\gamma^0(\epsilon_q - g_{\omega q}\omega - \tau_{3q}g_{\rho q}\rho) - \vec{\gamma}\cdot\vec{p} - (m_q - g_{\sigma q}\sigma) - U(r)]\psi_q(\vec{r}) = 0$$

$$U(r) = \frac{1}{2}(1+\gamma^0)(ar^2 + V_0)$$

$$V_0 = -62.257187\ \text{MeV}$$
$$a = 0.534296\ \text{fm}^{-3}$$

Parameter fixing

$$M_N = 939\ \text{MeV}$$
$$r_N = 0.87\ \text{fm}.$$

***Step 2: Effective Lagrangian for nucleon many-body system (N + σ,ω,ρ):***

$$\mathcal{L} = \overline{\psi}\left(i\gamma_\mu\partial^\mu - M_N^* - g_{\omega N}\omega\gamma^0 - g_{\rho N}\rho\tau_3\gamma^0\right)\psi - \frac{1}{2}(\nabla\sigma)^2 - \frac{1}{2}m_\sigma^2\sigma^2 - \frac{1}{3}g_2\sigma^3 - \frac{1}{4}g_3\sigma^4$$
$$+\frac{1}{2}(\nabla\rho)^2 + \frac{1}{2}m_\rho^2\rho^2 + \frac{1}{2}(\nabla\omega)^2 + \frac{1}{2}m_\omega^2\omega^2 + \frac{1}{2}g_{\rho N}{}^2\rho^2\Lambda_v g_{\omega N}{}^2\omega^2,$$

Guichon, Toki, Shen, Providência, Stone, Thomas, etc (1978-

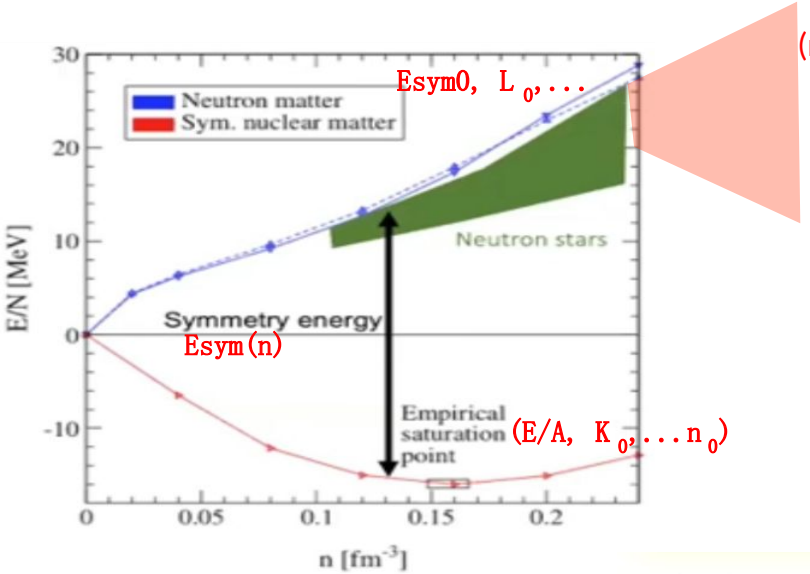
| $L$ [MeV] | $g_{\sigma q}$ | $g_{\omega q}$ | $g_{\rho q}$ | $g_2$ [fm$^{-1}$] | $g_3$ | $\Lambda_v$ |
|---|---|---|---|---|---|---|
| 20 | 3.8620366 | 2.9174838 | 6.9588083 | 14.6179599 | -66.3442468 | 1.1080665 |
| 40 | 3.8620366 | 2.9174838 | 5.4129448 | 14.6179599 | -66.3442468 | 0.7693664 |
| 60 | 3.8620366 | 2.9174838 | 4.5830609 | 14.6179599 | -66.3442468 | 0.4306662 |
| 80 | 3.8620366 | 2.9174838 | 4.0459574 | 14.6179599 | -66.3442468 | 0.0919661 |

Parameter fixing

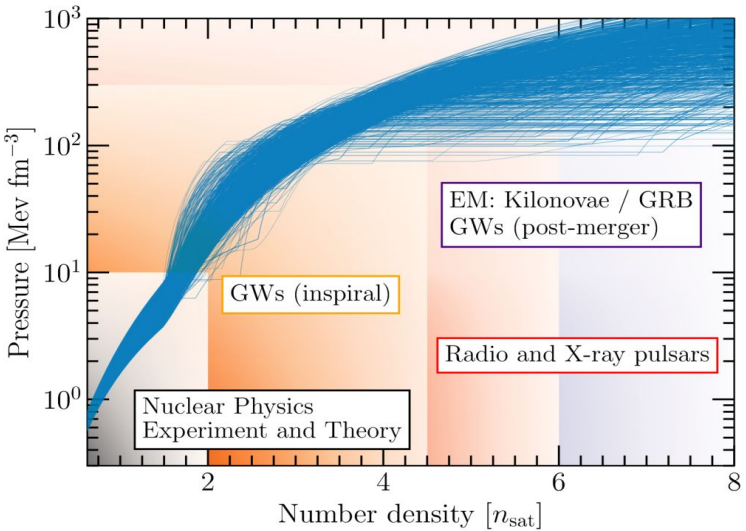
| $\rho_0$ [fm$^{-3}$] | $E/A$ [MeV] | $K$ [MeV] | $E_{\rm sym}$ [MeV] | $L$ [MeV] | $M_N^*/M_N$ / |
|---|---|---|---|---|---|
| 0.16 | -16 | 240 | 31 | 20/40/60/80 | 0.77 |

*1802.05510*

# Span uncertainty in EOS at supranuclear density




($n_{trans}$, $\Delta\varepsilon$, $c_{QM}$)




2205.08513

$$\begin{cases} E/A(n,0) = E_0/A + \dfrac{1}{18}K_0\dfrac{n-n_0}{n_0} + \ldots \\ E_{\rm sym}(n) = E^0_{\rm sym} + \dfrac{1}{3}L_0\dfrac{n-n_0}{n_0} + \ldots \end{cases}$$

$$\begin{cases} p(\mu_B) = A\mu_B^{1+1/c^2_{\rm QM}} - B \\ \mu_B(p) = [(p+B)/A]^{c^2_{\rm QM}/(1+c^2_{\rm QM})} \\ n(\mu_B) = (1+1/c^2_{\rm QM})A\mu_B^{1/c^2_{\rm QM}} \end{cases}$$

$$B = (\varepsilon_{\rm trans} + \Delta\varepsilon - c^{-2}_{\rm QM}\, p_{\rm trans})/(1+c^{-2}_{\rm QM})$$

| | $K_0$ | $E^0_{\rm sym}$ | $L_0$ | $m^*_0/m_N$ | $n_t/n_0$ | $\mu_{\rm crit}$ | $\Delta\varepsilon/\varepsilon_t$ | $c_s^2$ |
|---|---|---|---|---|---|---|---|---|
| prior | U(220, 280) | U(30, 35) | U(20, 120) | U(0.65, 0.8) | U(1, 4) | / | U(0, 2) | U(1/3, 1) |

full parameter space rom 1/sqrt(3) (the conformal limit in perturbative QCD matter) to 1 (the causal limit)

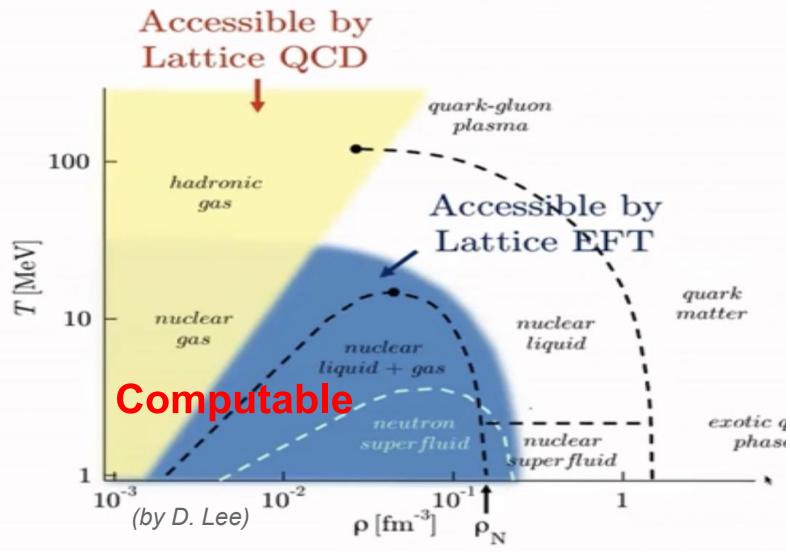
# Constraint on the pressure at densities ~1-3$n_0$ effectively tightened

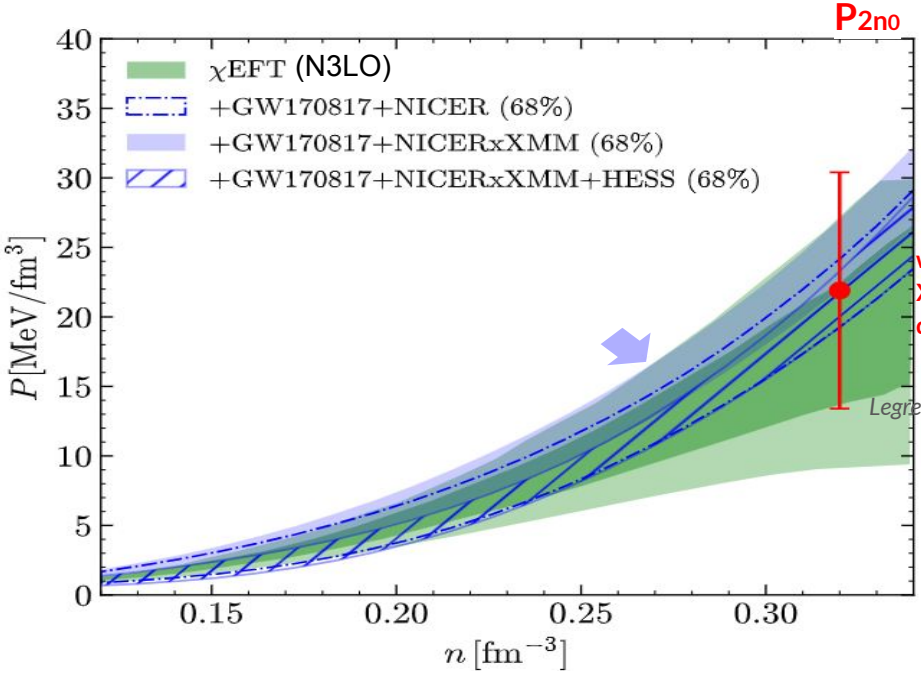
PHYSICAL REVIEW D **109,** 123005 (2024)

**Thermal x-ray studies of neutron stars and the equation of state**

Zhiqiang Miao,[1,2] Liqiang Qi,[3] Juan Zhang,[3] Ang Li,[2,*] and Mingyu Ge[3,†]
[1]*Tsung-Dao Lee Institute, Shanghai Jiao Tong University, Shanghai 201210, China*
[2]*Department of Astronomy, Xiamen University, Xiamen 361005, China*
[3]*Key Laboratory of Particle Astrophysics, Institute of High Energy Physics, Chinese Academy of Sciences, Beijing 100049, China*

2402.02799




Plus HESS data: Enlargement of the EOS parameter space.

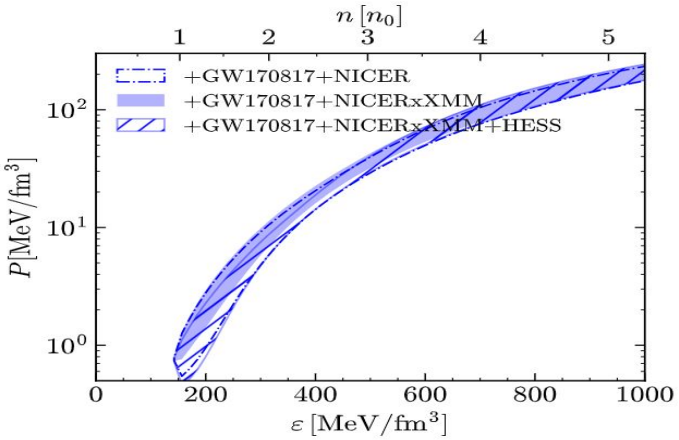
# Neutron stars vs. Hybrid stars

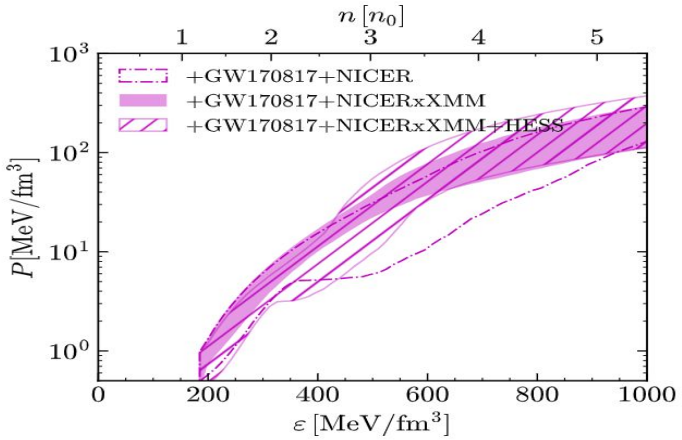
1σ credible intervals of HSs are **much larger** than those of pure NSs;

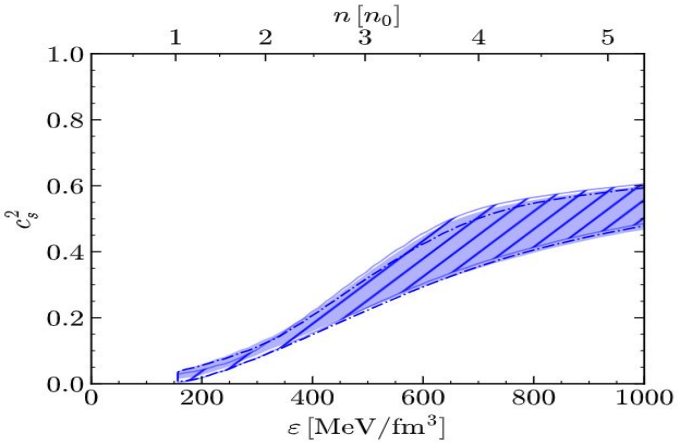
**Similar** results for $R_{1.4}$ (~12 km) are found for both pure NSs and HSs: **Need to degeneracies and identify potential phase transitions.**

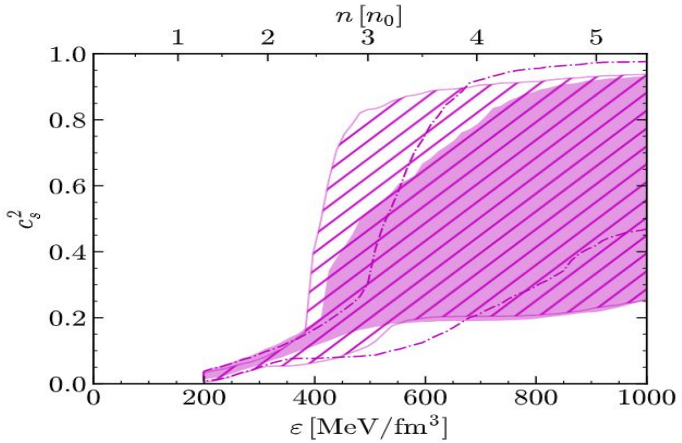
| | $R_{1.4}$ |
|---|---|
| NS (w.o. XMM) | $12.24^{+0.49}_{-0.36}$ |
| NS (with XMM) | $12.82^{+0.36}_{-0.46}$ |
| NS (plus HESS) | $12.11^{+0.29}_{-0.26}$ |
| HS (w.o. XMM) | $11.69^{+0.75}_{-0.63}$ |
| HS (with XMM) | $12.85^{+0.45}_{-0.51}$ |
| HS (plus HESS) | $12.20^{+0.35}_{-0.47}$ |

2402.02799



# Results on nuclear matter parameters and the phase transition: GW + X-ray (NICER⨯XMM+ HESS)

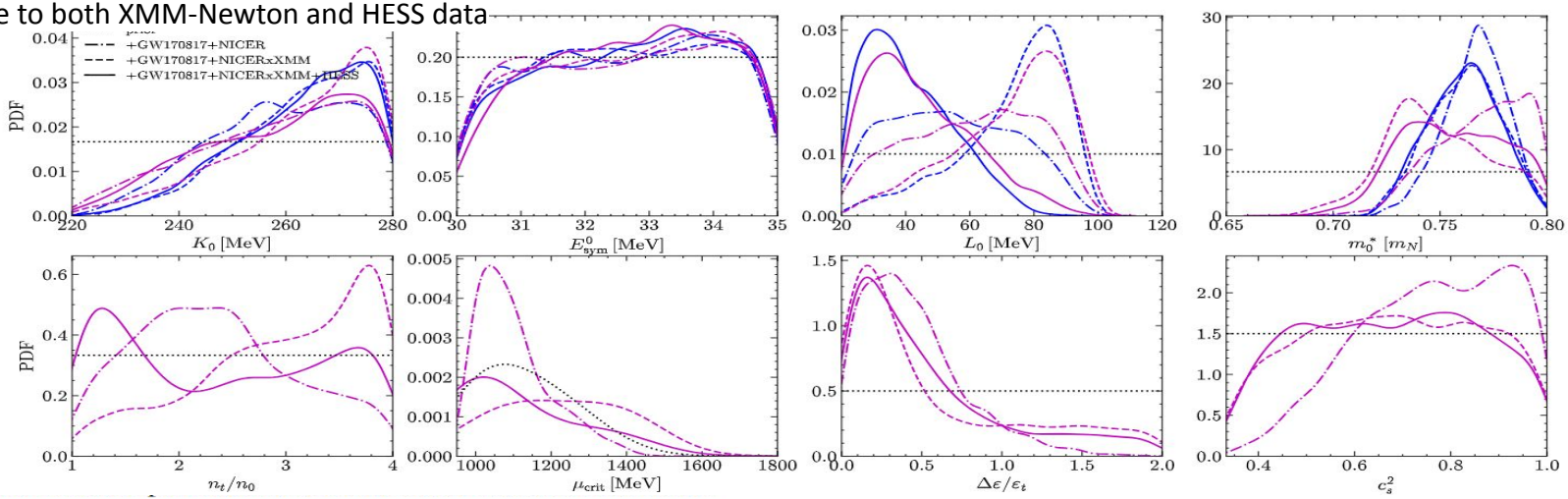
2402.02799

$K_0$ is more sensitive to XMM-Newton data

$L_0$ is more sensitive to both XMM-Newton and HESS data

$K_0$, $Esym0$, $L_0$, . . .

$n_{trans}$, $\Delta\varepsilon$, $c_{QM}$, . . .




| | $K_0$ | $E^0_{\rm sym}$ | $L_0$ | $m_0^*/m_N$ | $n_t/n_0$ | $\mu_{\rm crit}$ | $\Delta\varepsilon/\varepsilon_{\rm t}$ | $c_s^2$ |
|---|---|---|---|---|---|---|---|---|
| prior | U(220, 280) | U(30, 35) | U(20, 120) | U(0.65, 0.8) | U(1, 4) | / | U(0, 2) | U(1/3, 1) |
| NS (w.o. XMM) | $259.63^{+13.92}_{-15.53}$ | $32.64^{+1.58}_{-1.77}$ | $53.56^{+23.05}_{-21.02}$ | $0.77^{+0.01}_{-0.02}$ | / | / | / | / |
| NS (with XMM) | $265.06^{+10.70}_{-14.85}$ | $32.62^{+1.61}_{-1.65}$ | $77.50^{+10.90}_{-21.34}$ | $0.76^{+0.02}_{-0.02}$ | / | / | / | / |
| NS (plus HESS) | $265.11^{+10.23}_{-15.81}$ | $32.76^{+1.51}_{-1.74}$ | $38.39^{+17.68}_{-11.41}$ | $0.76^{+0.02}_{-0.02}$ | / | / | / | / |
| HS (w.o. XMM) | $259.85^{+14.01}_{-18.83}$ | $32.66^{+1.61}_{-1.79}$ | $62.13^{+20.44}_{-25.00}$ | $0.77^{+0.02}_{-0.03}$ | $2.28^{+0.92}_{-0.72}$ | $1078.82^{+125.22}_{-69.80}$ | $0.38^{+0.35}_{-0.24}$ | $0.77^{+0.16}_{-0.18}$ |
| HS (with XMM) | $265.86^{+10.25}_{-17.86}$ | $32.73^{+1.52}_{-1.77}$ | $76.60^{+12.79}_{-23.76}$ | $0.75^{+0.03}_{-0.02}$ | $3.11^{+0.69}_{-1.05}$ | $1311.67^{+1063.26}_{-239.94}$ | $0.31^{+0.95}_{-0.22}$ | $0.68^{+0.21}_{-0.21}$ |
| HS (plus HESS) | $260.99^{+13.15}_{-19.61}$ | $32.73^{+1.51}_{-1.63}$ | $41.74^{+20.48}_{-13.27}$ | $0.76^{+0.03}_{-0.02}$ | $2.38^{+1.21}_{-1.11}$ | $1101.85^{+1198.91}_{-116.53}$ | $0.37^{+0.65}_{-0.26}$ | $0.68^{+0.20}_{-0.21}$ |

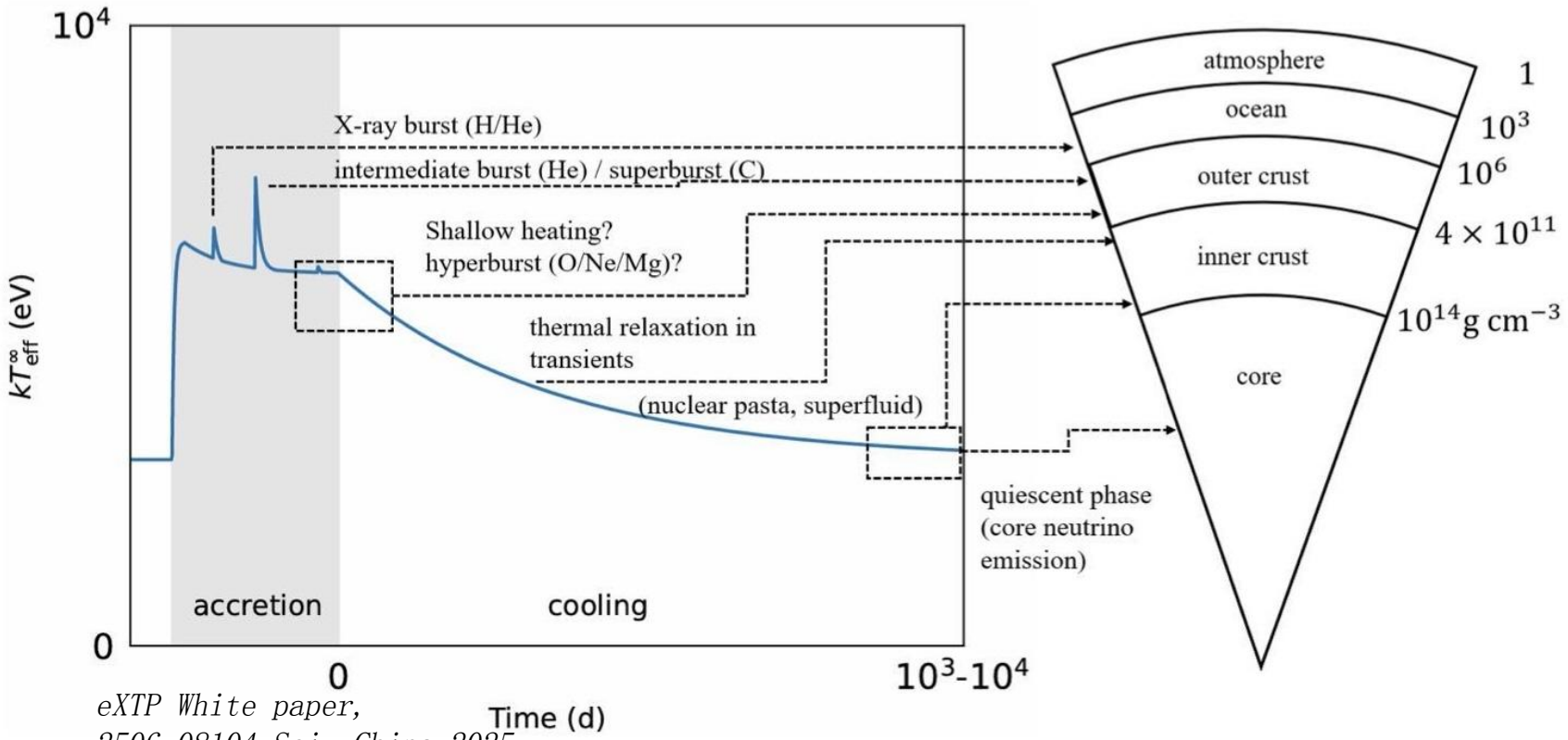
# Outline

- Intro. on neutron stars and M, R study
- Observations and multi-messenger constraints
- **Prospects and opportunities**

# Neutron star cross section and thermal light curve



eXTP will build an extensive sample of high-precision data for exploring the thermal and rotational evolution of NSs.




*eXTP White paper, 2506.08104 Sci. China 2025*

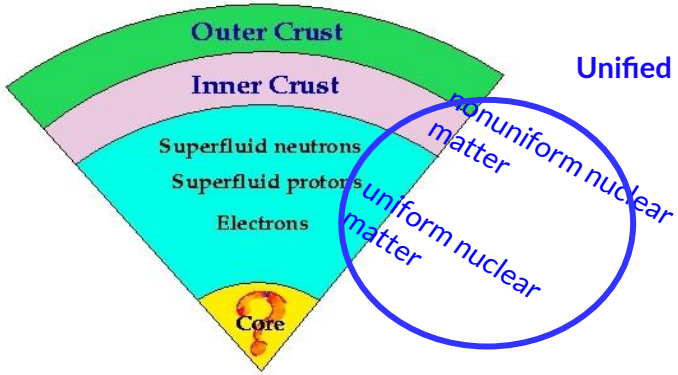
PHYSICAL REVIEW D **112,** 043018 (2025)

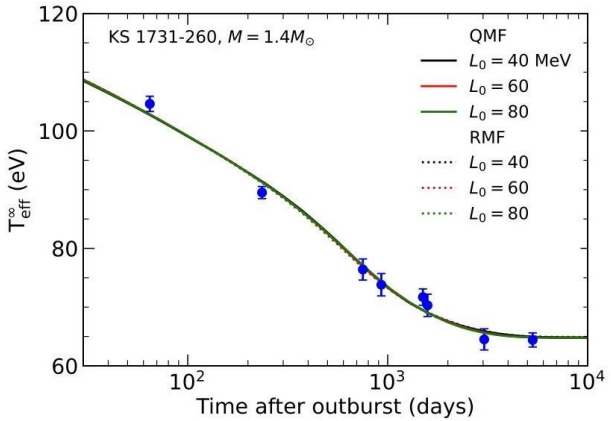
# Unified quark mean-field equation of state for neutron star matter: Static and dynamic properties

Zhonghao Tu,[1] Xiangdong Sun,[1] Shuochong Han,[1] Zhiqiang Miao,[2] and Ang Li[1,*]
[1]*Department of Astronomy, Xiamen University, Xiamen 361005, China*
[2]*Tsung-Dao Lee Institute, Shanghai Jiao Tong University, Shanghai 201210, China*

(Received 8 May 2025; accepted 24 July 2025; published 13 August 2025)

We construct a set of unified equations of state based on the quark mean-field (QMF) model, calibrated to different values of nuclear symmetry energy slope at the saturation density ($L_0$), with the aim of exploring both the static properties and dynamical behavior of neutron stars (NSs), and building a coherent picture of their internal structure. We assess the performance of these QMF models in describing the mass-radius relation, the cooling evolution of isolated NSs and x-ray transients, and the instabilities (e.g., the r mode). In comparison to relativistic mean-field (RMF) models formulated at the hadronic level, the QMF model predicts heavier nuclear clusters and larger Wigner-Seitz cell sizes in the NS crust, while the density of the free neutron gas remains largely similar between the two approaches. For the cooling of isolated NSs, the thermal evolution is found to be insensitive to both the many-body model and the symmetry energy slope in the absence of the direct Urca (dUrca) process. However, when rapid cooling via the dUrca process is allowed, in the case of large $L_0$ values (e.g., $L_0 \gtrsim 80$ MeV) in our study, the QMF model predicts a longer thermal relaxation time. Both the QMF and RMF models can reproduce cooling curves consistent with observations of x-ray transients (e.g., KS 1731-260) during their crustal cooling phase, although stellar parameters show slight variations depending on the model and symmetry energy slope. Within our unified framework, a larger $L_0$ value generally results in a wider instability window, while increasing the stellar mass tends to suppress the instability window. We also provide simple power-law parametrizations that quantify the dependence of bulk and shear viscosities on the symmetry energy slope for nuclear matter at saturation density.



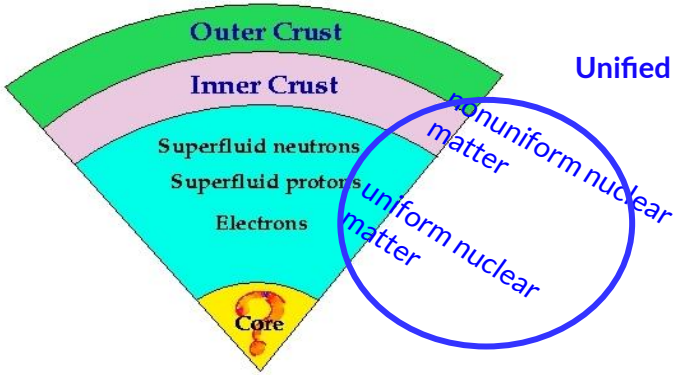



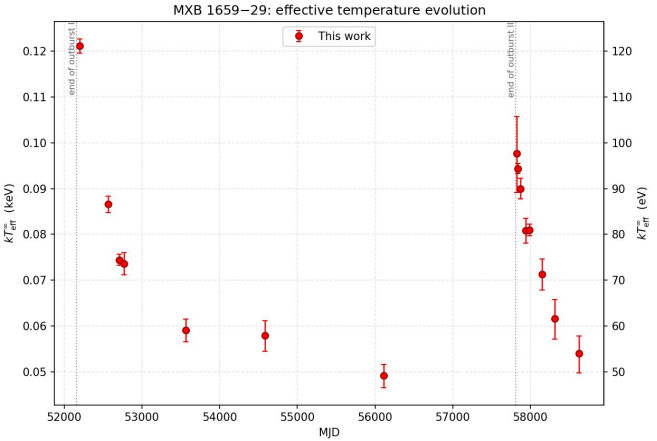
# Unified quark mean-field equation of state for neutron star matter: Static and dynamic properties

Zhonghao Tu,[1] Xiangdong Sun,[1] Shuochong Han,[1] Zhiqiang Miao,[2] and Ang Li[1,*]
[1]*Department of Astronomy, Xiamen University, Xiamen 361005, China*
[2]*Tsung-Dao Lee Institute, Shanghai Jiao Tong University, Shanghai 201210, China*

(Received 8 May 2025; accepted 24 July 2025; published 13 August 2025)

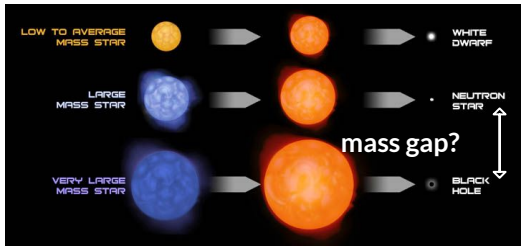
We construct a set of unified equations of state based on the quark mean-field (QMF) model, calibrated to different values of nuclear symmetry energy slope at the saturation density ($L_0$), with the aim of exploring both the static properties and dynamical behavior of neutron stars (NSs), and building a coherent picture of their internal structure. We assess the performance of these QMF models in describing the mass-radius relation, the cooling evolution of isolated NSs and x-ray transients, and the instabilities (e.g., the r mode). In comparison to relativistic mean-field (RMF) models formulated at the hadronic level, the QMF model predicts heavier nuclear clusters and larger Wigner-Seitz cell sizes in the NS crust, while the density of the free neutron gas remains largely similar between the two approaches. For the cooling of isolated NSs, the thermal evolution is found to be insensitive to both the many-body model and the symmetry energy slope in the absence of the direct Urca (dUrca) process. However, when rapid cooling via the dUrca process is allowed, in the case of large $L_0$ values (e.g., $L_0 \gtrsim 80$ MeV) in our study, the QMF model predicts a longer thermal relaxation time. Both the QMF and RMF models can reproduce cooling curves consistent with observations of x-ray transients (e.g., KS 1731-260) during their crustal cooling phase, although stellar parameters show slight variations depending on the model and symmetry energy slope. Within our unified framework, a larger $L_0$ value generally results in a wider instability window, while increasing the stellar mass tends to suppress the instability window. We also provide simple power-law parametrizations that quantify the dependence of bulk and shear viscosities on the symmetry energy slope for nuclear matter at saturation density.

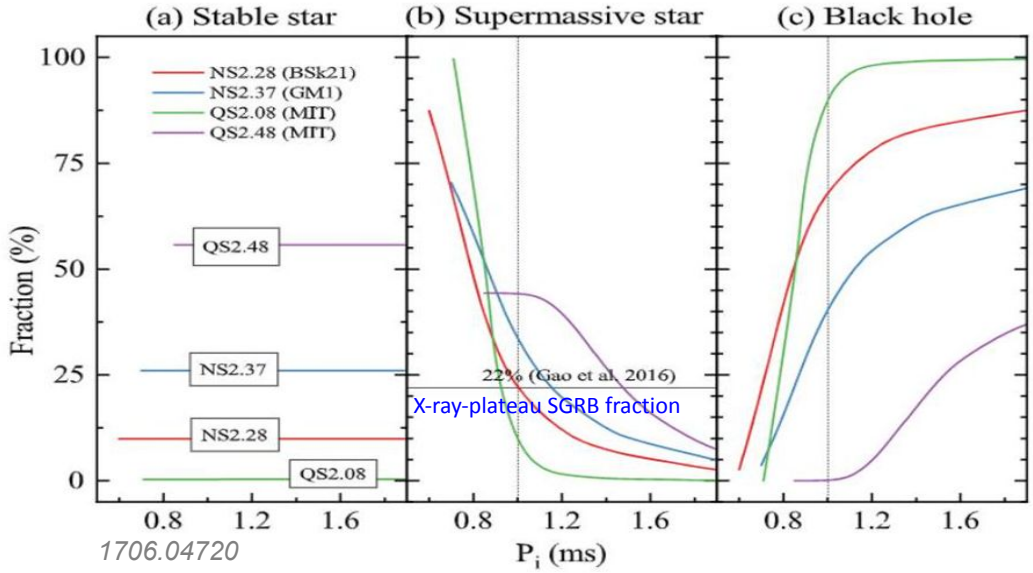


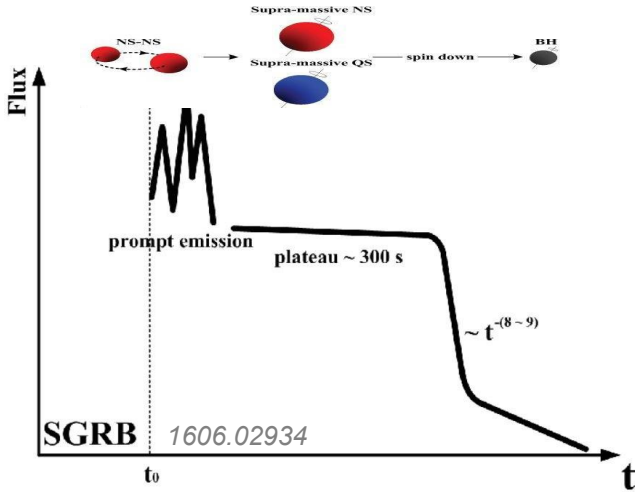



# The maximum mass and merger remants

EM counterparts and post-merger GW observations can provide hints on merger remants, therefore provide information about the maximum mass and high-density stiffness of the EOS (SWOM, EP, etc).




How well the underlying EOS would reconcile is largely determined by the static maximum mass of that EOS.

# Multi-wavelength studies working with other WGs

Five Hundred Metre Aperture Radio Telescope (FAST)

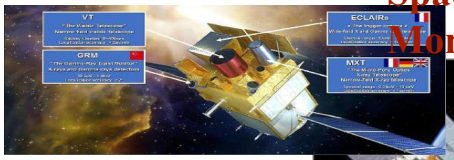



NanShan 25-m Radio Telescope



- More samples;
- Better ppm modeling;
- Mass;
- Distance;
- etc

Space Variable Objects Monitor (SVOM)










Fermi Gamma-ray Space Telescope




Parkes 64-m Radio Telescope




MeerKAT radio telescope





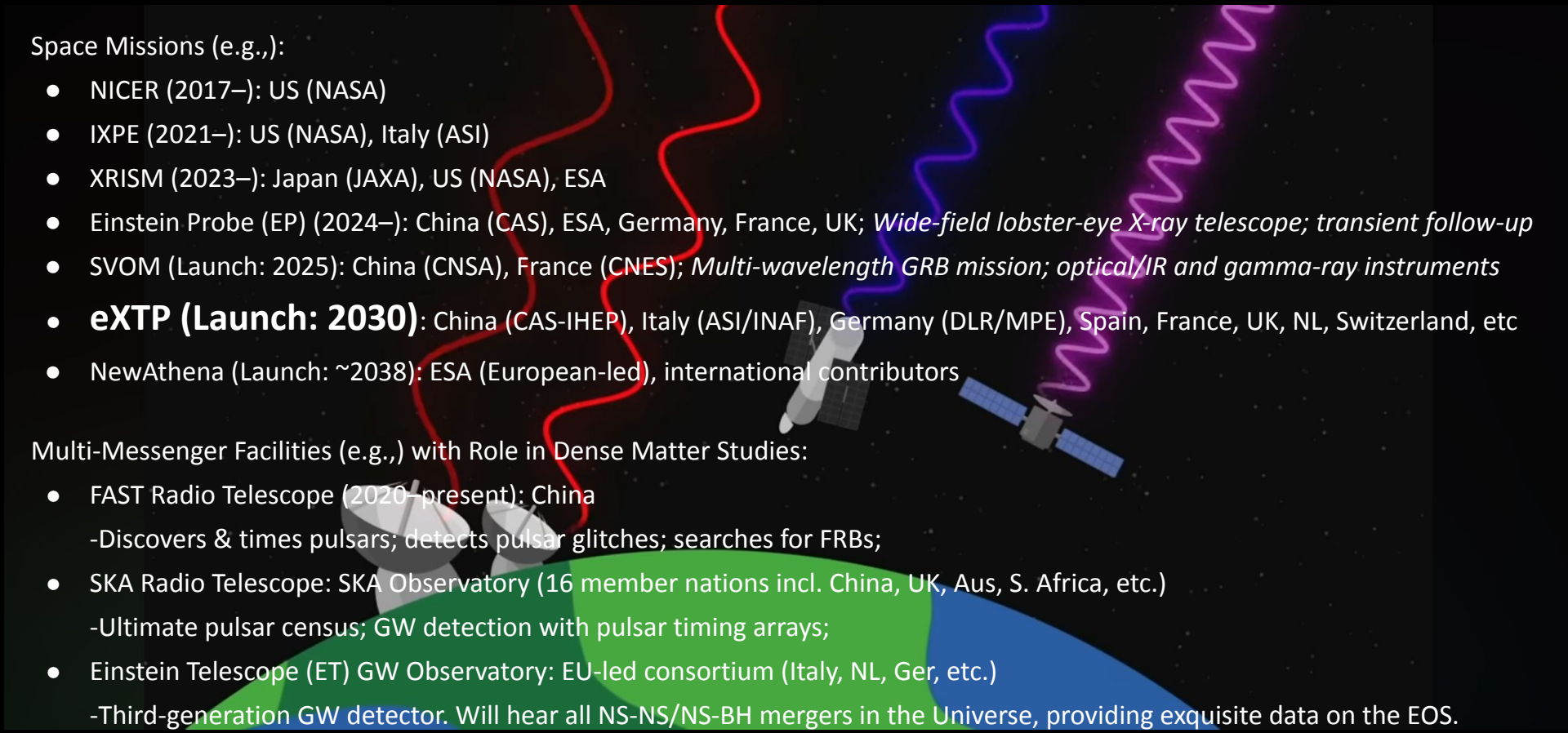

**Radio** observations are essential for measuring spin, timing behavior, binary parameters, and, in favorable systems, masses through relativistic orbital effects;

**Optical** observations can constrain binary companions, distances, and orbital inclinations;

**High-energy** missions provide information about transient activity, magnetospheric emission, and merger counterparts

…

# Synchronized multi-messenger campaigns for next decade



Space Missions (e.g.,):

- NICER (2017–): US (NASA)
- IXPE (2021–): US (NASA), Italy (ASI)
- XRISM (2023–): Japan (JAXA), US (NASA), ESA
- Einstein Probe (EP) (2024–): China (CAS), ESA, Germany, France, UK; *Wide-field lobster-eye X-ray telescope; transient follow-up*
- SVOM (Launch: 2025): China (CNSA), France (CNES); *Multi-wavelength GRB mission; optical/IR and gamma-ray instruments*
- **eXTP (Launch: 2030)**: China (CAS-IHEP), Italy (ASI/INAF), Germany (DLR/MPE), Spain, France, UK, NL, Switzerland, etc
- NewAthena (Launch: ~2038): ESA (European-led), international contributors

Multi-Messenger Facilities (e.g.,) with Role in Dense Matter Studies:

- FAST Radio Telescope (2020–present): China
  -Discovers & times pulsars; detects pulsar glitches; searches for FRBs;
- SKA Radio Telescope: SKA Observatory (16 member nations incl. China, UK, Aus, S. Africa, etc.)
  -Ultimate pulsar census; GW detection with pulsar timing arrays;
- Einstein Telescope (ET) GW Observatory: EU-led consortium (Italy, NL, Ger, etc.)
  -Third-generation GW detector. Will hear all NS-NS/NS-BH mergers in the Universe, providing exquisite data on the EOS.

# Neutron-star structure is an old problem that is newly ripe for progress !

SCIENCE CHINA
Physics, Mechanics & Astronomy

• Invited Review •
Special Issue: Exploration of the Extreme Universe with the eXTP Mission

November 2025 Vol. 68 No. 11: 119503
https://doi.org/10.1007/s11433-025-2761-4

Thank you !

## Dense matter in neutron stars with eXTP

Ang Li[1*], Anna L. Watts[2], Guobao Zhang[3], Sebastien Guillot[4], Yanjun Xu[5], Andrea Santangelo[6,5], Silvia Zane[7], Hua Feng[5], Shuang-Nan Zhang[5], Mingyu Ge[5], Liqiang Qi[5], Tuomo Salmi[8], Bas Dorsman[2], Zhiqiang Miao[9], Zhonghao Tu[1], Yuri Cavecchi[10], Xia Zhou[11], Xiaoping Zheng[12], Weihua Wang[13], Quan Cheng[12], Xuezhi Liu[12], Yining Wei[12], Wei Wang[14], Yujing Xu[1,15], Shanshan Weng[15], Weiwei Zhu[16,17], Zhaosheng Li[18], Lijing Shao[19], Youli Tuo[6], Akira Dohi[20,21], Ming Lyu[18], Peng Liu[1], Jianping Yuan[11], Mingyang Wang[1], Wenda Zhang[16], Zexi Li[5], Lian Tao[5], Liang Zhang[5], Hong Shen[22], Constança Providência[23], Laura Tolos[24,25], Alessandro Patruno[24,25], Li Li[26], Guozhu Liu[27], Kai Zhou[28], Lie-Wen Chen[29], Yizhong Fan[30], Toshitaka Kajino[31,32,33], Dong Lai[9,34], Xiangdong Li[35], Jie Meng[36], Xiaodong Tang[37], Zhigang Xiao[38], Shaolin Xiong[5], Renxin Xu[18,39], Shan-Gui Zhou[26], David R. Ballantyne[40], G. Fiorella Burgio[41], Jérôme Chenevez[42], Devarshi Choudhury[2], Anthea F. Fantina[43], Duncan K. Galloway[44,45], Francesca Gulminelli[46], Kai Hebeler[47], Mariska Hoogkamer[2], Jorge E. Horvath[48], Yves Kini[2], Aleksi Kurkela[49], Manuel Linares[50,10], Jérôme Margueron[51,52], Melissa Mendes[47], Micaela Oertel[53], Alessandro Papitto[54], Juri Poutanen[55], Nanda Rea[24,25], Achim Schwenk[47], Xin-Ying Song[5], Isak Svensson[47], David Tsang[56], Aleksi Vuorinen[8,57], Nils Andersson[58], M. Coleman Miller[59], Luciano Rezzolla[60], Jirina R. Stone[61], and Anthony W. Thomas[62]

With the timely efforts of eXTP, we will be able to advance the understanding of several key questions central to the long-standing challenge of determining the EOS of dense matter.

- How does pressure depend on density, composition and temperature, that is, the EOS, and how does this influence the properties of NSs?
- What is the observational evidence of the presence of heavy baryons or deconfined quarks at the extreme densities in NS cores, and what are the implications?
- What is the role of superfluidity in regulating thermal evolution and glitch behavior?
- How does nuclear pasta vary throughout the deep layers of NS crusts?
- What is the maximum possible rotation speed of a NS?



https://indico.global/event/15804/




Spectral-Timing-Polarimetry in the eXTP Era



31 August – 2 September, 2026
Turku, Finland